International Journal of Intelligent Information Systems
2025, Vol. 14, No. 2, pp. 26-43
https://doi.org/10.11648/j.ijiis.20251402.12

Research Article

Multi-strategy Enhanced Dwarf Mongoose Optimization Algorithm for Microgrid Optimal Scheduling Problem

Weiping Meng[1], **Shijian Chen**[1], **Yongquan Zhou**[1, 2, *]

[1]College of Artificial Intelligence, Guangxi Minzu University, Nanning, China

[2]Guangxi Key Laboratories of Hybrid Computation and IC Design Analysis, Nanning, China

Abstract

A microgrid is an autonomous system that can realize self-control, protection, and management and is composed of distributed power sources, energy storage devices, loads, and control and protection devices. To achieve low operation costs, this paper a multi-strategy enhanced dwarf mongoose optimization algorithm (EDMO) for microgrid scheduling problem is proposed. In EDMO, the convergence speed is accelerated by introducing the golden Sine strategy, which generally makes it difficult to find new excellent solutions at a later stage, lead to a reduction in the population diversity and limiting the development capability, as well as introducing adaptive t-distribution variation to increase the population diversity and the introduction L évy flight to enhance the algorithm's ability to jump out of the local optimum. The EDMO was compared with other nine algorithms applied to the microgrid optimal scheduling problem. The experimental results show that the proposed EDMO can achieved the lowest total cost, exhibits good performance and robustness, and is an effective method for solving the microgrid scheduling problem.

Keywords

Microgrid Optimal, Dwarf Mongoose Optimization, Golden Sine Strategy, Adaptive t-distribution Mutation, L évy Flight, Metaheuristic Optimization

1. Introduction

With the transformation of the economic growth model of modern society, the structure of electric power production is also changing, along with the upgradation of industrial and energy structures. In recent years, the global emphasis on new energy has increased, which is in line with the development of the times to eliminate the dependence on a single source of energy but also to contribute to the improvement of the ecological environment. In the face of changes in the power supply and demand, microgrids [1-3] have become the choice for power systems to cope with energy security and low-carbon development. Microgrids involve the comprehensive utilization of wind, solar, natural gas, electricity, and other energy sources, and their scheduling problem is complex. Microgrid optimal scheduling refers to the reduction of operating costs, improvement of new energy utilization, enhancement of the stability of the power grid, reduction of environmental pollution, energy loss, etc., by rationally arranging the power of each power source and load of the microgrid under the premise of ensuring the safe and stable operation of the system.

The microgrid scheduling problem is a classical unit-combination (UC) problem. So far, there are many

*Corresponding author: yongquanzhou@126.com (Yongquan Zhou)

Received: 20 April 2025; **Accepted:** 3 May 2025; **Published:** 3 June 2025

Copyright: © The Author(s), 2025. Published by Science Publishing Group. This is an **Open Access** article, distributed under the terms of the Creative Commons Attribution 4.0 License (http://creativecommons.org/licenses/by/4.0/), which permits unrestricted use, distribution and reproduction in any medium, provided the original work is properly cited.

scholars have conducted research on microgrid (MG) scheduling problems, such as Lagrangian relaxation [4], mixed-integer linear programming [5], metaheuristic optimization algorithms [6], et al. In [7], an improved quantum particle swarm optimization (QPSO) using a differential evolutionary algorithm was proposed, the experiments show that the improved QPSO has better performance and is more suitable than the QPSO and CLQPSO to solve the demand problem of microgrids. In [8], an improved real-coded genetic algorithm (GA) and enhanced mixed-integer linear programming (MILP)-based, developed GA-based, and MILP-based optimizers were proposed for application to a test microgrid model under different operating strategies. The experimental results show that voltage and load violations can be corrected very accurately. In [8], a hybrid improved GSA-PSO was proposed by combining the gravitational search algorithm (GSA) and particle swarm optimization (PSO) algorithms (MGSA-PSO), which implements and analyzes load scheduling optimization. Experimental results demonstrate the effectiveness of the proposed scheme by analyzing the effects of different numbers of electric vehicles and different charging modes. In [9], a chaotic cuckoo search SVR (SVRCCS) model based on the tent chaotic mapping function was proposed. The numerical results from the dataset tests show that the proposed SVRCCS model outperforms other alternative models. In [10], an improved mayfly algorithm incorporating Levy flights is proposed, the experimental results demonstrate that the proposed IMA algorithm can solve the CEED problem in grid-connected microgrids. In [11], a cuckoo search algorithm (CSA) was used to optimize the economic dispatch of microgrids, the experimental results show that CSA has good global convergence and provides a better optimal solution and emission costs. In [12], an enhanced population-aware particle swarm optimization (QS-PSO) was used to determine the full-cycle optimal scheduling solution for microgrids, the experimental results demonstrate the effectiveness of the proposed scheduling model and QS-PSO application. In [13], a metaheuristic adaptive elephant swarm optimization (SA-EHO) was proposed for the implementation of an ideal scheduling model for microgrids (MGs) with EVs and RESs. The experimental results demonstrate that the proposed algorithm performed well. In [14], a variant of the Non-dominated Sorting Genetic Algorithm (NSGA)-II algorithm was used along with the introduction of an external penalty function to deal with the constraints and facilitate the solution of the multi-objective optimization model. The proposed algorithm was applied to the dynamic economic dispatch model of a microgrid. The economy of the proposed scheme was verified by comparing its economic dispatch effects under different operating conditions. In [15], a BSA based on an adaptive taxing flight strategy (LF-BSA) was proposed, the experimental results verify the feasibility of LF-BSA and the effectiveness of multi-objective optimization. In [16], the Whale Optimization Algorithm (WOA) was used to perform all ELDs, emission scheduling, and CEEDs on islanded and renewable energy-integrated microgrids, the experimental results demonstrate that the proposed method outperforms other optimization techniques. In [17], a symbiotic organism search (SOS)-based staging algorithm and an improved multi-intelligent actor (MA) consensus algorithm (IMACA) were proposed, the experimental results verify that the proposed algorithm has superior performance and can obtain the most economically efficient solution. In [18], an improved PSO algorithm with adaptive inertia weights and shrinkage factors was proposed, the results show that the improved PSO algorithm effectively reduces the comprehensive objective cost and achieves better optimization results. In [19], an improved butterfly optimization algorithm (IBOA) based on a partial tent chaotic map, Cauchy variation, and simplex method was proposed, the experimental results show that the IBOA can effectively reduce the system cost of electricity, promote the effective utilization of renewable energy, and improve the operational stability of the microgrid cluster system. In [20], Giza pyramid construction (GPC) is proposed to realize the optimal design of isolated microgrids. Net current cost (NPC), levelized cost of energy (LCOE), loss of power probability and availability index are used as objective functions. In [21], an improved mayfly optimization algorithm was proposed for solving microgrid problems. These results were compared with those of recent state-of-the-art algorithms using the same microgrid model. Experimental results show that the proposed algorithm is competitive and robust.

This paper a multi-strategy enhanced dwarf mongoose optimization algorithm (EDMO) for microgrid scheduling problem is proposed. The main contributions are as follows:

(1) The dwarf mongoose optimization algorithm was enhanced with the golden sine strategy, adaptive t-distribution variational strategy, and Lévy flight strategy.

(2) A multi-strategy enhanced dwarf mongoose optimization algorithm (EDMOA) was proposed.

(3) Comparison with well-known algorithms, and it is experimentally verified that the proposed EDMOA performs better than the other algorithms.

(4) The EDMOA was successfully applied to solve the microgrid optimal scheduling problem.

2. Microgrid Model

In this section, the mathematical model of the microgrid optimal dispatch problem is proposed which includes the wind turbine, photovoltaic, diesel generator, micro gas turbine, battery, and the objective functions. The main objective of optimal microgrid scheduling is to minimize the operating cost of the microgrid in grid-connected mode.

2.1. Wind Turbine Model

A wind turbine (WT) [22], which is mathematically mod-

eled as shown in Eq. (1):

$$P_{WT}=\begin{cases}0, & v<v_{ci}\\ av^3+bv^2+cv+d, & v_{ci}\le v\le v_r\\ P_r, & v_r<v<v_{co}\\ 0, & v\ge v_{co}\end{cases} \quad (1)$$

In Eq. (1), PWT is the output power of the wind turbine, P_r is the rated power of the wind turbine, v_{ci} is the cut-in wind speed of the wind turbine, v_r denotes the rated wind speed of the wind turbine, and v_{co} denotes the cut-out wind speed of the wind turbine, a, b, c, and d denote the wind speed parameters.

2.2. Photovoltaic Power Generation Model

The mathematical model of the PV output power [23] is given by Eq. (2).

$$P_{pv}=R_{pv}q_{pv}\frac{I_T}{I_{STC}}\left[1+\alpha_p(T_c-T_{stc})\right] \quad (2)$$

where P_{pv} denotes the PV power output, R_{pv} denotes the PV power output under the standard test, q_{pv} denotes the derating coefficient of the PV, I_T denotes the actual solar irradiation intensity, I_{STC} denotes the solar irradiation intensity under the standard test, αp denotes the temperature coefficient of the PV panels, Tc denotes the temperature of the PV panels in the current time interval, and *Tstc* denotes the temperature of the PV cells under the standard test. PV cell temperature under test.

2.3. Diesel Generator Model

The diesel generator [24] is a type of power machine that uses diesel fuel and a diesel engine as the prime mover to drive the generator to generate electricity. The entire set is generally composed of a diesel engine, generator, control box, fuel tank, starting and control batteries, protection device, emergency cabinet, and other components. Diesel generators are economical and efficient power generation equipment with a wide range of applications in modern society. The model is given in Eq. (3).

$$\begin{cases}C_{DM}(t)=K_{DM}P(t)\\ C_{DF}(t)=\alpha P_{DE}^2(t)+\beta P_{DE}(t)+\gamma\\ C_{DN}(t)=\sum_{k=1}^{n}(C_k\gamma_{DE,k})P_{DE}(t)\\ \alpha=0.00011,\beta=0.1801,\lambda=6\end{cases} \quad (3)$$

where $C_{DM}(t)$, $C_{DF}(t)$, and $C_{DN}(t)$ denote the operation and maintenance, fuel, and pollution treatment costs of the diesel generator at moment t, respectively. $P_{DE}(t)$ denotes the power generation of the diesel generator at time t, K_{DM} denotes the coefficient of operation and maintenance cost of the diesel generator, denotes the amount of release of the k pollutants generated by the operation of the diesel generator, *Ck* denotes the treatment of the k pollutant cost coefficient, and denotes the coefficient of the diesel generator.

2.4. Micro Turbine Model

A microturbine (MT) [25, 26] is a gas turbine with a power range of 25–300kW. It is characterized by its small size, light weight, high power density, low noise, low emission, high reliability, and low maintenance cost compared to conventional gas turbines and has broad application prospects in the fields of distributed power generation, standby power generation, cogeneration, and mobile power. The working principle of a micro gas turbine is the same as that of a traditional gas turbine, which converts the thermal energy generated by fuel combustion into mechanical energy and then converts it into electric energy through a generator. It is mainly composed of four core components: compressor, combustion chamber, turbine, and generator. The output power of the micro gas turbine was adjustable and exhibited a high response speed. The model is given in Eq. (4).

$$\eta_{MT}(t)=0.0753\left[\frac{P_{MT}(t)}{65}\right]^3-0.3095\left[\frac{P_{MT}(t)}{65}\right]^2+0.4174\frac{P_{MT}(t)}{65}+0.1068 \quad (4)$$

where $\eta_{MT}(t)$ represents the operating efficiency of the micro-gas turbine, and is the active output power of the micro-gas turbine. The operation and maintenance costs, pollutant treatment costs and fuel costs will be generated during the operation of the micro-gas turbine, and the model is shown in Eq. (5).

$$\begin{cases}C_{MM}(t)=K_M P_{MT}(t)\\ C_{MF}(t)=\frac{C}{LHV}\times\frac{P_{MT}(t)}{\eta_{MT}(t)}\\ C_{MN}(t)=\sum_{k=1}^{n}(C_k\gamma_{mt,k})P_{MT}(t)\end{cases} \quad (5)$$

where $C_{MM}(t)$, $C_{MF}(t)$, and $C_{MN}(t)$ denote the operation and maintenance, fuel, and pollution treatment costs of the diesel generator at moment t, respectively. $P_{MT}(t)$ denotes the power generation of the diesel generator at moment t, K_M denotes the operation and maintenance cost coefficient of the diesel generator, K_M denotes the amount of k pollutant releases generated by the operation of the diesel generator, C_k denotes the cost factor for treating k pollutant releases, and C_k denotes the cost factor for treating *k* pollutants. Cost coefficient of pollutant treatment.

2.5. Battery Model

Storage batteries work by using electrochemical reactions to convert chemical energy into electrical energy [27]. When the battery is discharged, the electrochemical reaction causes the active substances inside the battery to change, thereby releasing electrical energy. When the battery was recharged, the electrical energy provided by the external power supply restored the active material inside the battery to its original state. The role of the battery as a reserve energy, in the case of renewable energy, cannot meet the load of the microgrid system for the system energy supply, thereby stabilizing the system power supply and ensuring stable and safe operation of the system. The model is given in Eq. (6).

$$SOC(t)=\begin{cases} SOC(t-1)+\dfrac{1}{\eta^{-}}P_{bess}(t), P_{bess}(t)\le 0 \\ SOC(t-1)+\dfrac{1}{\eta^{+}}P_{bess}(t), P_{bess}(t)>0 \end{cases} \tag{6}$$

where SOC (t) indicates the remaining capacity of the battery at moment t and P_{bess} (t) indicates the charging and discharging power of the battery at time t. When the result is positive, it indicates charging, and when the result is negative, it indicates discharging, which indicates the charging efficiency, which indicates the discharging efficiency.

2.6. Constraints

(1) Power-balance constraint

Power constraint is one of the most important constraints in power system dispatching, which can ensure the safe and stable operation of the power grid and improve its economic operation of the power grid. This requires the sum of the generation power and load power of each node in the grid to be equal. The model is given in Eq. (7).

$$P_{pv}(t)+P_{WT}(t)+P_{grid}(t)+P_{DE}(t)+P_{MT}(t)+P_{bess}(t)=P_{L}(t) \tag{7}$$

(2) Diesel generator output constraints:

The diesel generator output constraints refer to the diesel generator set in the operation process, and its output does not exceed a certain limit. The role of diesel generator output constraints is to ensure the safe operation of diesel generator sets, extend the service life of diesel generator sets, and improve their economic efficiency of diesel generator sets. The diesel generator output constraints are an important constraint in the operation of diesel generator sets, and the safe, reliable, and economic operation of diesel generator sets plays a vital role. The model is given in Eq. (8).

$$\begin{cases} P_{DE}^{\min}(t)\le P_{DE}(t)\le P_{DE}^{\max}(t) \\ \left|P_{DE}(t)-P_{DE}(t-1)\right|\le r_{DE} \end{cases} \tag{8}$$

(3) The micro gas turbine Output constraints

The output force constraint of a micro gas turbine is an important constraint in the operation process of a micro gas turbine and plays a vital role in the safe, reliable, and economical operation of micro gas turbines. The model is given in Eq. (9).

$$\begin{cases} P_{MT}^{\min}(t)\le P_{MT}(t)\le P_{MT}^{\max}(t) \\ \left|P_{MT}(t)-P_{MT}(t-1)\right|\le r_{MT} \end{cases} \tag{9}$$

(4) Transmission power constraints for the contact lines

The transmission power constraint of the contact line refers to the fact that the transmission power of the contact line does not exceed a certain limit under normal operation conditions. The model is given in Eq. (10).

$$P_{grid}^{\min}(t)\le P_{grid}(t)\le P_{grid}^{\max}(t) \tag{10}$$

(5) Energy storage device constraints

The energy storage device constraint refers to the fact that during the operation of the energy storage device, parameters such as output power, charging and discharging power, voltage, and current must not exceed certain limit values to ensure the safe operation of the energy storage device. The model is given in Eq. (11).

$$\begin{cases} P_{bess}^{\min}(t)\le P_{bess}(t)\le P_{bess}^{\max}(t) \\ SOC^{\min}(t)\le SOC(t)\le SOC^{\max}(t) \end{cases} \tag{11}$$

In Eqs. (7)-(11), $P_{DE}^{\max}(t)$, $P_{DE}^{\min}(t)$ represent the upper and lower limits of the output power of the diesel engine, and $P_{MT}^{\max}(t)$, $P_{MT}^{\min}(t)$ represent the upper and lower limits of the output power of the micro-gas turbine; r_{DE}, r_{MT} represent the upper limit of the climbing power of the diesel generator and the upper limit of the climbing power of the micro-gas turbine; and $P_{grid}^{\max}(t)$, $P_{grid}^{\min}(t)$ represent the upper and lower limits of the power transmitted by the contact line, respectively; $P_{bess}^{\max}(t)$, $P_{grid}^{\min}(t)$ denote the upper and lower limits of the output power of the energy storage device, and the positive value indicates the power input, while the negative value indicates the power output; $SOC_{max}(t)$ and $SOC_{min}(t)$ denote the upper and lower limits of the energy storage capacity at the time of t, respectively.

2.7. Objective Function of the Microgrid Optimal Dispatch Problem

(1) The microgrid operating cost

The mathematical model of the microgrid operating cost is expressed by Eq. (12).

$$f_1 = \sum_{t=1}^{T} C_{grid}(t) + C_{MT}(t) + C_{DE}(t) \tag{12}$$

$$\begin{cases} C_{grid}(t) = C_{buy}(t) + C_{sell}(t) \\ C_{buy}(t) = c_{buy}(t) P_{buy}(t) \\ C_{sell}(t) = c_{sell}(t) P_{sell}(t) \\ C_{DE}(t) = C_{DM}(t) + C_{DF}(t) \\ C_{MT}(t) = C_{MM}(t) + C_{MF}(t) \end{cases}$$

where $C_{grid}(t)$, $C_{bess}(t)$, $C_{MT}(t)$, and $C_{DE}(t)$ denote the total cost of interaction between the microgrid and the main grid at moment t, the cost of maintenance of the energy storage, the total operating cost of the microgas turbine, and the total operating cost of the diesel generator, respectively; $P_{bess}(t)$ denotes the power of the energy storage at moment t. $P_{sell}(t)$ and $_{Pbuy}(t)$ denote the power sold and purchased at moment t for the microgrid and the large grid, respectively; and c_{buy} (t) and c_{sell} (t) denote the price of electricity purchased and the price of electricity sold at moment t for the microgrid and the large grid, respectively.

(2) The microgrid Environmental protection cost

The model of the environmental protection cost of microgrid is given by Eq. (13).

$$\begin{cases} f_2 = \sum_{t=1}^{T} C_{GN}(t) + C_{MN}(t) + C_{DN}(t) \\ C_{GN}(t) = \sum_{t-1}^{T} (C_k \gamma_{grid,k}) P_{buy}(t) \end{cases} \tag{13}$$

where $C_{GN}(t)$ denotes the pollutant treatment cost of the large power grid, denotes the release amount of pollutants of type k generated by the operation of the large power grid, and C_k denotes the cost coefficient of treating pollutants of type k.

(3) Objective function of the microgrid optimal scheduling.

The objective function of the microgrid optimal scheduling problem model is to minimize the total cost, including the operating and environmental costs. The model is given in Eq. (14).

$$Z = f_1 + f_2 \tag{14}$$

3. Dwarf Mongoose Optimization Algorithm

The Dwarf Mongoose Optimization (DMO) Algorithm is proposed by Jeffrey O. in 2022 [28]. It is inspired by the group foraging behavior of dwarf mongooses and mainly simulates the foraging, scouting, and babysitting behaviors of dwarf mongooses.

3.1. Population Initialization

The initialization of the DMO starts with the selection of candidate meerkat individuals that are randomly generated between the upper and lower bounds of the given problem. The population is initialized as shown in Eq. (15):

$$X = \begin{bmatrix} X_{1,1} & X_{1,2} & \cdots & X_{1,d} \\ X_{2,1} & X_{2,2} & \cdots & X_{2,d} \\ \cdots & \cdots & \cdots & \cdots \\ X_{N,1} & X_{N,2} & \cdots & X_{N,d} \end{bmatrix} \tag{15}$$

where X denotes the candidate solution, $X_{i,j}$ denotes the position of the ith mongoose in the jth dimension, and the mathematical model is given by Eq. (16). N and d denote the population and dimension sizes of the problem, respectively.

$$X_{i,j} = unifrnd(lb, ub, d) \tag{16}$$

where *unifrnd* is used to generate uniformly distributed random numbers and *ub* and *lb* denote the upper and lower bounds of the given problem, respectively. d denotes the dimensional size of the problem.

3.2. Alpha Group

The foraging routes of the dwarf mongoose were determined by the alpha females produced in the alpha group. The probability that each female individual in the alpha group will become a leader is determined using Eq. (17):

$$\alpha = \frac{fit(i)}{\sum_{i=1}^{n} fit(i)} \tag{17}$$

The number of mongooses in the alpha group corresponds to the *n-bs*. Where *bs* is the number of babysitters; $fit(i)$ denotes the fitness value of the ith individual, the alpha female's vocalization that keeps the family within a path is denoted by *peep*. Each individual in the alpha group forages for food, and the formula for updating the location of the food source is shown in Eq. (18):

$$X_{i+1} = X_i + phi \times peep \times (X_i - X_k) \tag{18}$$

where $X_{i,j}$ denote the location of the new food source, X_i denotes the location of the ith individual, and phi is a random number between [-1, 1]; the female alpha keeps the whole group within a path by making a sound, denoted by "*peep*," and the value of *peep* is set to 2 in this paper. x_k denotes the alpha group of X_k denotes the attendant individuals in the alpha group.

Sleeping mounds are the resting places of the dwarf mongoose population and are calculated using the following

formula:

$$sm_i = \frac{fit(i+1) - fit(i)}{\max\left\{\left| fit(i+1), fit(i)\right|\right\}} \tag{19}$$

The formula for calculating the mean value of a sleep mound is as follows:

$$\phi = \frac{\sum_{i=1}^{n} sm_i}{n} \tag{20}$$

3.3. Scout Group

Members of the scouting group were responsible for finding the next sleeping mound, as the dwarf mongoose would not return to a place where it had previously slept, which ensured that territories were explored and that scouting and foraging took place simultaneously. This movement was modeled as an overall success or failure assessment for finding a new sleeping mound. In other words, this movement depends on the overall performance of the dwarf mongoose. The rationale is that if the dwarf mongoose colony forages far enough away, it will find a new sleep mound. The formula for updating the position of an individual in a scouting group is as follows.

$$X_{i+1} = \begin{cases} X_i - C \times phi \times r \times \left| X_i - \overrightarrow{M} \right| & if \ \ \phi_{i+1} > \phi_i \\ X_i + C \times phi \times r \times \left| X_i - \overrightarrow{M} \right| & else \end{cases} \tag{21}$$

where C denotes the parameter controlling the mobility of the dwarf meerkat population, which decreases linearly with the number of iterations, as shown in Eq. (22), *phi* is a random number between [-1, 1], r represents a random number between [0, 1], M is the direction vector determining the movement of the dwarf meerkat towards the new sleep mound, as shown in Eq. (23) and φ is given by Eq. (20).

$$C = (1 - \frac{t}{Max\_t})^{(2\frac{t}{Max\_t})} \tag{22}$$

where t denotes the number of iterations, and *Max_t* denotes the maximum number of iterations.

$$\overrightarrow{M} = \sum_{i=1}^{n} \frac{X_i - sm_i}{X_i} \tag{23}$$

where n denotes the number of members in the scout group, X_i denotes the position of the ith individual, and sm_i denotes the value of the sleep mound.

3.4. Babysitters Group

Babysitters are usually subordinate group members who stay with the pups and rotate periodically so that the alpha female can lead the rest of the group in daily foraging. The alpha female usually returns to the nurse the pups at midday and evening. The number of nannies depends on the size of the population, and they affect the algorithm by reducing the overall population size by a set percentage. This population was modeled by a percentage reduction in the number of nanny groups. The nanny exchange parameter was used to reset the scouting and food source information held by family members. The babysitter fitness weight was set to zero, which ensured that the alpha group's average weight was reduced in the next iteration, implying that the group's movement was impeded, thus emphasizing exploitation.

4. Enhanced Dwarf Mongoose Optimization Algorithm

4.1. Golden Sine Strategy

The Gold-SA [29] (Gold-SA) is proposed by Tanyildizi et al. in 2017, which is inspired by the sine function in mathematics. The advantages of gold-SA are fast convergence, good robustness, and ease of implementation. Gold-SA utilizes the sine function and the unit circle relationship to the unit circle to search for the unit circle. The position update formula is given in Eq. (24).

$$X_i(t+1) = X_i(t)\left|\sin(r_1)\right| - r_2 \sin(r_1)\left|D_i(t)x_1 - X_i(t)x_2\right| \tag{24}$$

where r_1 is the determining parameter of the moving distance of the next-generation individual, r_1 is a random number between [0, 2π], r_2 is the parameter that determines the moving direction of the next-generation individual, and the range of the value is [0, π]; and x_1, x_2 are the golden section coefficients, and their mathematical expressions are shown in Eq. (25).

$$\begin{cases} x_1 = a(1-t) + bt \\ x_2 = at + b(1-t) \end{cases} \qquad t = \frac{\sqrt{5}-1}{2} \tag{25}$$

where $a = -\pi$, $b = \pi$, and t is the golden fraction ratio.

4.2. Adaptive t-distribution Mutation Strategy

Adaptive t-distribution mutation [30] (ATS) is a mutation operator for optimization problems. It is a mutation operator based on *t*-distribution, in the iterative process of the algorithm, the parameter of the degrees of freedom of the

t-distribution will be adaptively adjusted according to the progress of the algorithm, in the early stage of the algorithm, *n* is smaller, the *t*-distribution of the *t*-distribution of the *t*-distribution of the tail is longer, with a larger jump ability, which is conducive to the algorithm to jump out of the local optimal solution. In the later stages of the algorithm, *n* is larger, and the *t*-distribution has a shorter tail, which has a strong local search ability and is conducive to the algorithm converging to the global optimal solution. The mathematical model is given by Eq. (26).

$$\begin{cases} freen = e^{4*(\frac{t}{T})^2} \\ trnd(freen) \end{cases} \tag{26}$$

where t denotes the current iteration number, T denotes the maximum iteration number, and $trnd()$ denotes the t-distribution.

4.3. Levy Flight Strategy

The Lévy flight is a heuristic strategy for solving optimization problems [31]. This method adopts a Lévy distribution to realize stochastic search, integrates short-range search and long-range exploration, effectively enhances the global search capability of the algorithm, and improves the efficiency of jumping out of the local optimum. The model is given in Eq. (27).

$$levy(d) \tag{27}$$

where d denotes the dimensions of the problem.

4.4. Location Update Methods for EDMO

(1) Position update method for the alpha group

After the introduction of the adaptive t-distribution variation strategy and Levy flight strategy, the position update method for the alpha group is given by Eq. (28).

$$X_{i+1} = X_i + trnd(freen) \times p \times peep \times (X_i - X_k) \times levy(d) \tag{28}$$

(2) Position updating method of the scout group

After the introduction of the adaptive t-distribution variation strategy and Levy flight strategy, the position update method of the reconnaissance group is given by Eq. (29) and Eq. (30).

$$X_{i+1} = X_i + trnd(freen) \times p \times peep \times (X_i - X_k) \times levy(d) \tag{29}$$

$$X_{i+1} = \begin{cases} X_i - trnd(freen) \times levy(d) \times C \times p \times r \times \left| X_i - \overrightarrow{M} \right| & if \ \ \phi_{i+1} > \phi_i \\ X_i + trnd(freen) \times levy(d) \times C \times p \times r \times \left| X_i - \overrightarrow{M} \right| & else \end{cases} \tag{30}$$

4.5. Proposed EDMO Algorithm

The golden sine strategy can be used to solve various continuous, discrete, and multi-objective optimization problems. It can effectively find the optimal or near-optimal solution to a problem. It exhibits the characteristics of fast convergence and good robustness. The dwarf Mongoose optimization algorithm was combined with the golden sine strategy, and the performance of the algorithm was improved by combining adaptive T-distribution variation and Levy flight. Table 1 and Figure 1 show the flow chart of the EDMO algorithm.

Table 1. *Pseudo code of EDMO algorithm.*

Pseudo-code of the EDMO	
1.	Initialization Set the Mongoose populations(search agents): *n* Set the number of babysitters: *bs* Set *n*=*n*-*bs* Set babysitter exchange parameters L Set the values of parameters *Max_t*, *t*, *N*
2.	Step 2. Main loop
3.	while $t \leq Max\_t$
4.	Calculate the value of *C* using Eq. (22)
5.	for *i* =1: nAlphaGroup
6.	Calculate the position X_{i+1} using Eq. (28) and ϕ_{i+1} using Eq. (20)
7.	Calculate the X_{i+1}'fitness and update the fit_best
8.	end

Pseudo-code of the EDMO

9. for i=1: nScout
10. Calculate the position X_{i+1} using Eq. (29) and ϕ_{i+1} using Eq. (20)
11. Calculate the sm_i using Eq. (19)
12. end
13. for i=1: nBabysitter
14. Exchange members of the babysitters group and alpha group. If $C > L$
15. End
16 for i=1: N
17 Calculate the position X_{i+1} using Eq. (24)
18. end while
19. Step 3. Return fit_best and *Xbest*

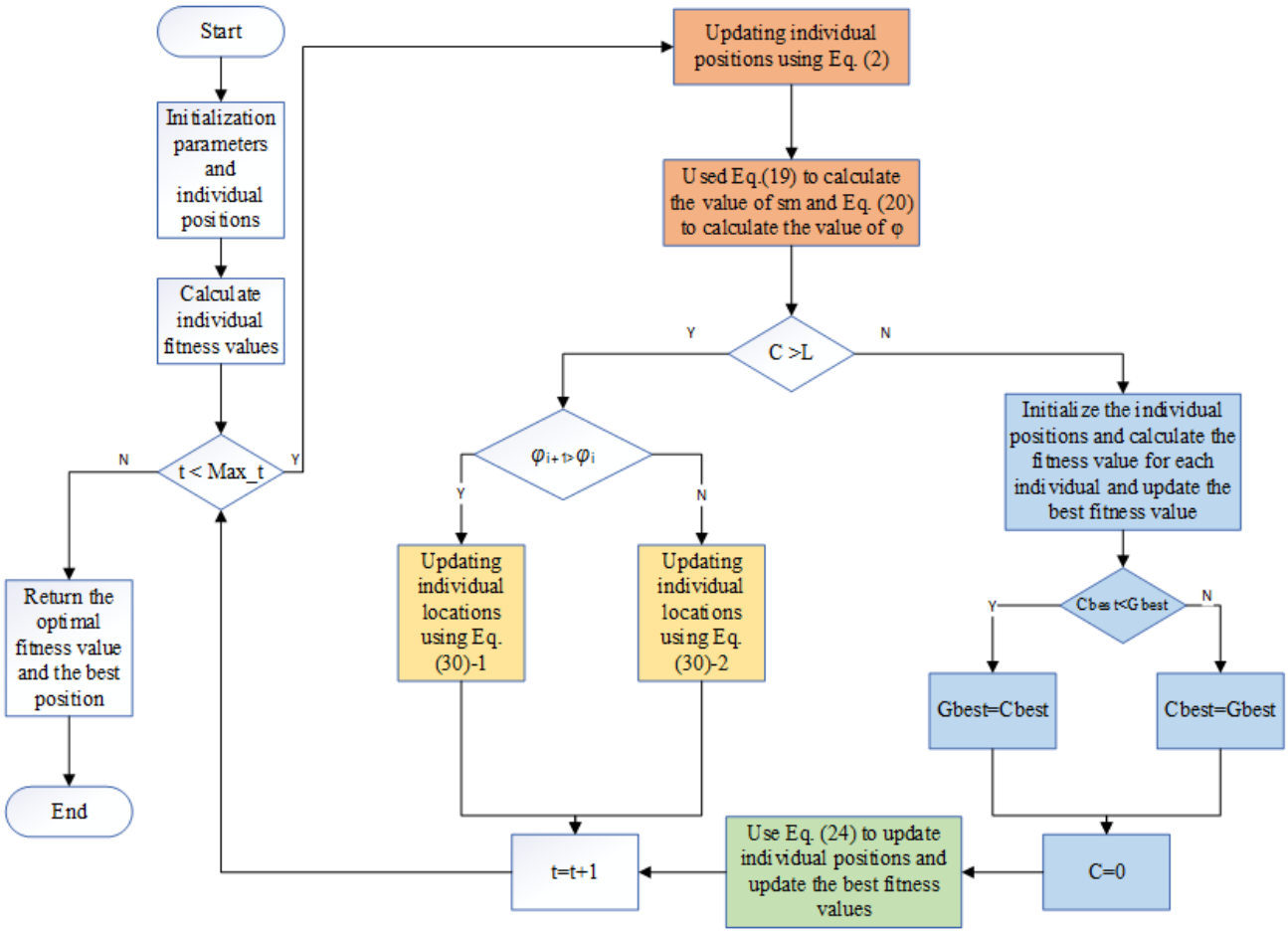

Figure 1. *Flowchart of EDMO.*

5. Experimental Results and Analysis

5.1. Experimental Parameter Settings

Table 2. Parameters set.

Parameters	Upper limit of power (/kW)	Lower limit of power (/kW)	Climbing power upper limit (/kW/min)	Unit cost of operation and maintenance (Yuan/kWh)
Diesel Generators	30	6	1.5	0.128
Turbine	100	0	0	0
Photovoltaic	50	0	0	0
Main network	30	-30	0	0
Gas turbine	30	3	1.5	0.0293

Table 3. Pollutant emission coefficients and treatment costs.

Pollutant types	Types	CO_2	SO_2	NO_3
Governance fees (yuan/kg)		0.023	6	8
Pollutant release coefficient (g/kWh)	PV	0	0	0
	WT	0	0	0
	DE	680	0.306	10.09
	Grid	889	1.8	1.6
	MT	724	0.0036	0.2

Table 4. Energy storage parameters.

Types	Parameters	Value	Parameters	Value
Storage battery	Maximum capacity (kWh)	150	Initial energy storage capacity (kWh)	50
	Minimum capacity (kWh)	5	Maximum output power (/kW)	30
	Maximum input power (/kW)	30	Charging and discharging power	0.9

The experimental parameters set are listed in the following Table 2. In addition, this experiment uses MATLAB2021b, and a Windows 10 64-bit operating system PC with an Intel Core i7-9700 processor @3.00GHz and 16.0 GB RAM served as the experimental platform. The proposed DMOWOA parameter settings: n=50, bs=3, Max_t=1500, t=0, N=20; L=8. Cited references related to all algorithm parameters compared.

Table 5. Price list for buying and selling electricity.

Time	Buying electricity prices from the power grid (Yuan/degree)	Selling electricity prices to the power grid (Yuan/degree)
1	0.3800	0.3600
2	0.3800	0.3600
3	0.3800	0.3600

Time	Buying electricity prices from the power grid (Yuan/degree)	Selling electricity prices to the power grid (Yuan/degree)
4	0.3800	0.3600
5	0.3800	0.3600
6	0.3800	0.3600
7	0.8200	0.3600
8	0.8200	0.3600
9	0.8200	0.3600
10	1.3500	0.3600
11	1.3500	0.3600
12	1.3500	0.3600
13	1.3500	0.3600
14	1.3500	0.3600
15	0.8200	0.3600
16	0.8200	0.3600
17	0.8200	0.3600
18	1.3500	0.3600
19	1.3500	0.3600
20	1.3500	0.3600
21	1.3500	0.3600
22	1.3500	0.3600
23	0.3800	0.3600
24	0.3800	0.3600

5.2. Experimental Results Analysis

To verify the performance of EDMO in solving the microgrid optimal scheduling problem, EDMO was compared with the ABC [32], AOA [33], ChOA [34], GWO [35], MPA [36], PSO [37], SA [38], SWO [39], and WOA [40]. For fairness of the comparison, the maximum number of iterations for each algorithm was 15000 and 20 independent runs. Four indicators were selected as statistical criteria: minimum (Min), maximum (Max), mean (Mean), and standard deviation (SD). Wilkerson's signed rank test [41] was used for statistical analysis, with the symbol "+" indicating better than the comparison algorithm, the symbol "-" indicating worse than the comparison algorithm, and the symbol "≈" indicates the comparison algorithm.

Table 6 shows the statistics of the results of 20 independent runs of each algorithm, from Table 5.6, it shows that EDMO is ranked first in the minimum value, followed by SA, SWO, PSO, DMO, MPA, ABC, GWO, WOA, ChOA, and the worst one is AOA. EDMO is ranked first in terms of the maximum value, mean value, and standard deviation. This verifies that EDMO outperformed the compared algorithms.

Table 6. *Indicators of solution results of each algorithm.*

Algorithm	Min	Max	Mean	SD
EDMO	48659.468	48756.429	48705.649	19.611
DMO	48978.638	49119.950	49055.622	39.066
ABC	49461.484	49663.384	49584.333	59.591
AOA	102158.293	114684.488	109974.031	2841.778
ChOA	96666.137	104215.045	100533.918	1746.452
GWO	50218.807	51519.838	50694.681	364.571
MPA	49101.468	50538.822	49382.887	297.005
PSO	48763.043	49027.188	48878.559	67.604
SA	48682.557	48858.215	48771.110	49.252
SWO	48697.393	49037.761	48814.131	98.056
WOA	77814.013	93653.616	86675.015	5214.493

The results of Wilkerson's signed-rank test are shown in Table 7, from which it can be seen that EDMO is statistically superior to DMO, ABC, AOA, ChOA, GWO, MPA, PSO, SA, SWO, and WOA. Therefore, it can be statistically verified that EDMO is an effective method for solving the optimal dispatch problem of microgrid.

Table 7. *Details of Wilkerson test for EDMO and other algorithms.*

Algorithms	R^+	R^-	*P*-value	±/≈
EDMO vs DMO	210	0	6.757e-08	+
EDMO vs ABC	210	0	6.757e-08	+
EDMO vs AOA	210	0	6.767e-08	+
EDMO vs ChOA	210	0	6.766e-08	+
EDMO vs GWO	210	0	6.757e-08	+
EDMO vs MPA	210	0	6.767e-08	+
EDMO vs PSO	210	0	6.767e-08	+
EDMO vs SA	191	19	2.220e-06	+
EDMO vs SWO	174	36	1.798e-05	+
EDMO vs WOA	210	0	6.767e-08	+

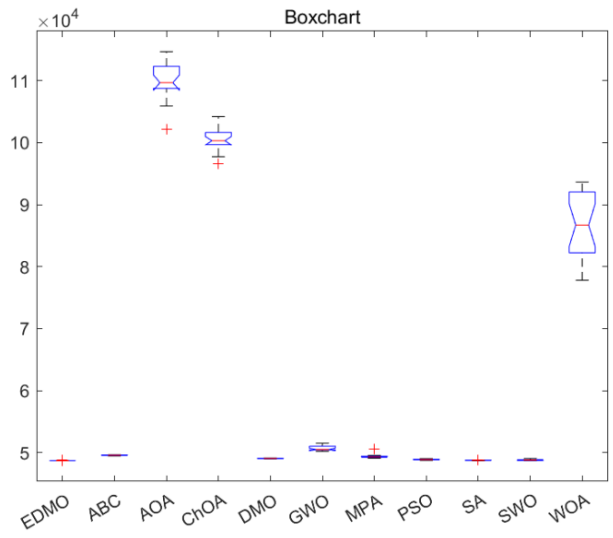

Figure 2. *Box diagram of each algorithm.*

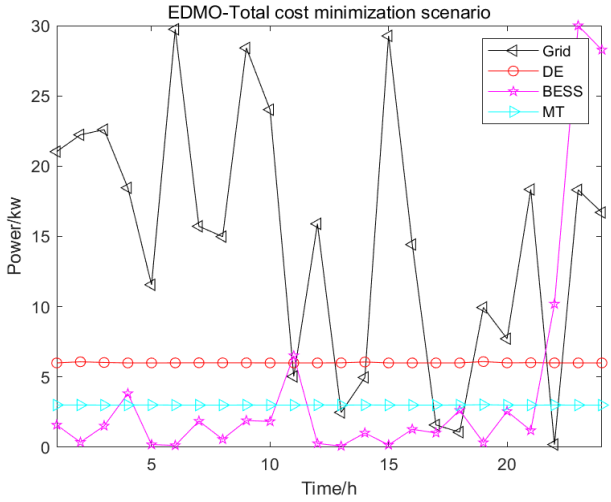

Figure 3. *Scheduling results for EDMO at the lowest total cost.*

Figure 2 shows the box-line plots of each algorithm, from which it can be seen that the data fluctuation of EDMO for 20 independent runs is very small, indicating that the algorithm is stable. This is followed by SA, DMO, and PSO. The data fluctuations of AOA, ChOA, and WOA were very large, indicating weak stability. Thus, the stability and robustness of EDMO were verified.

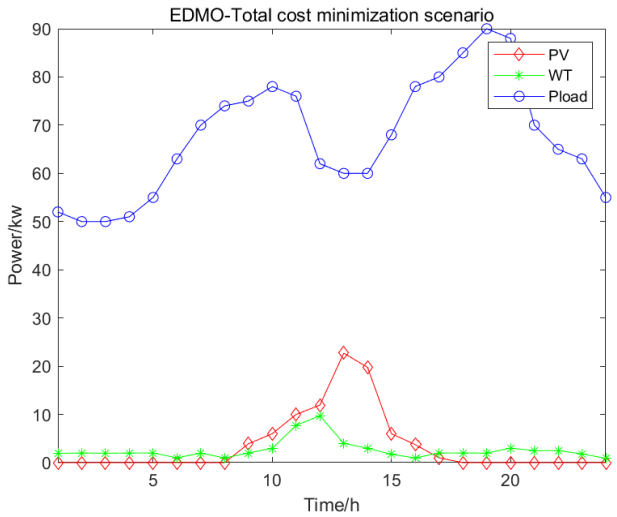

Figure 4. *Predicted EDMO values for PV, wind, and load power at lowest total cost.*

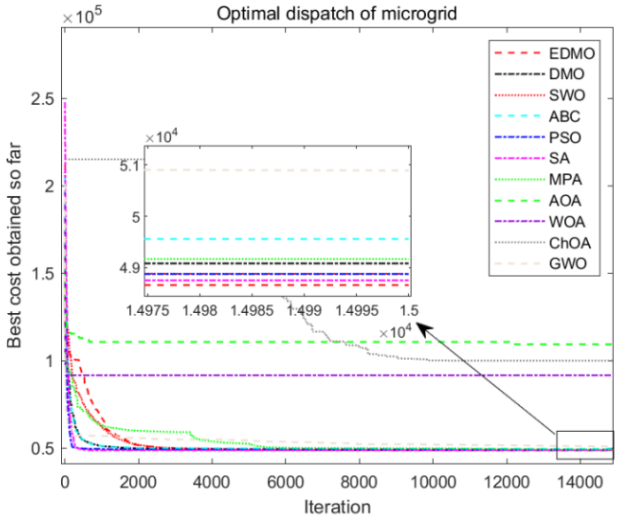

Figure 5. *Convergence curves for each algorithm.*

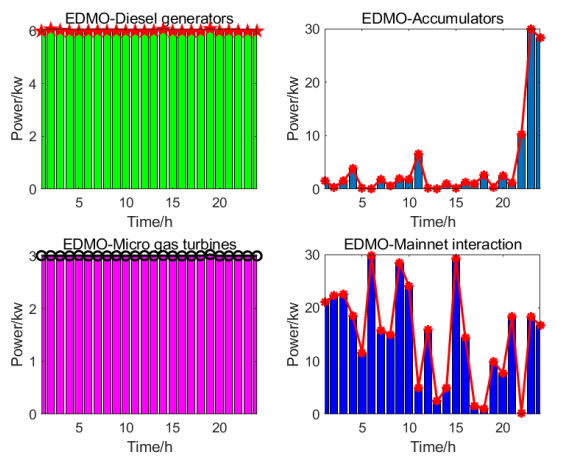

(a) EDMO

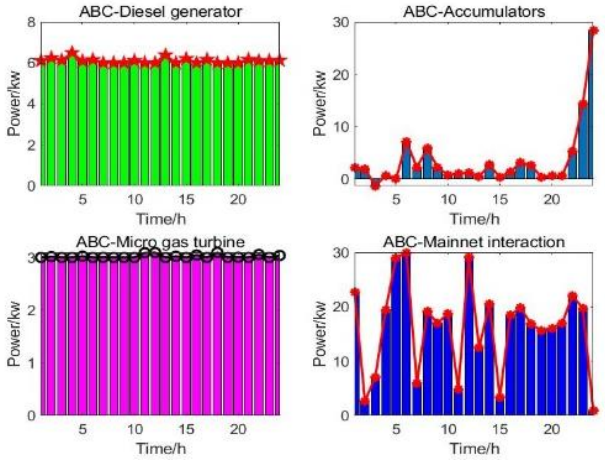

(b) ABC

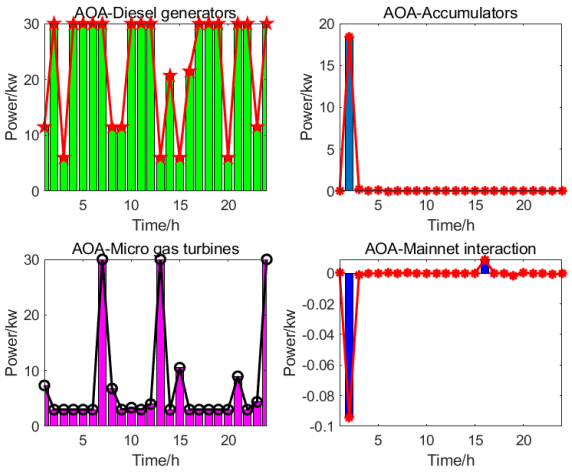

(c) AOA

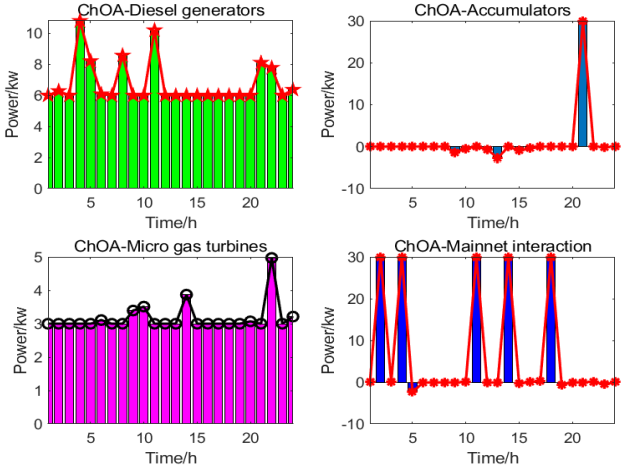

(d) ChOA

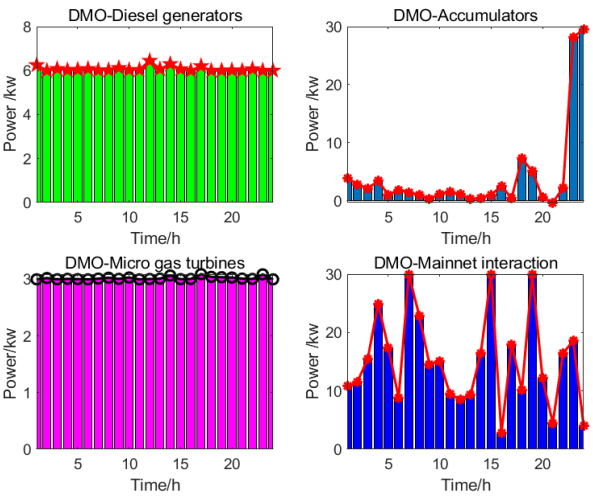

(e) DMO

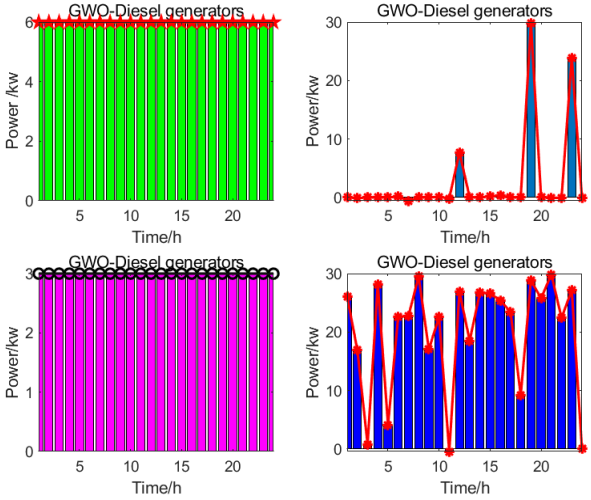

(f) GWO

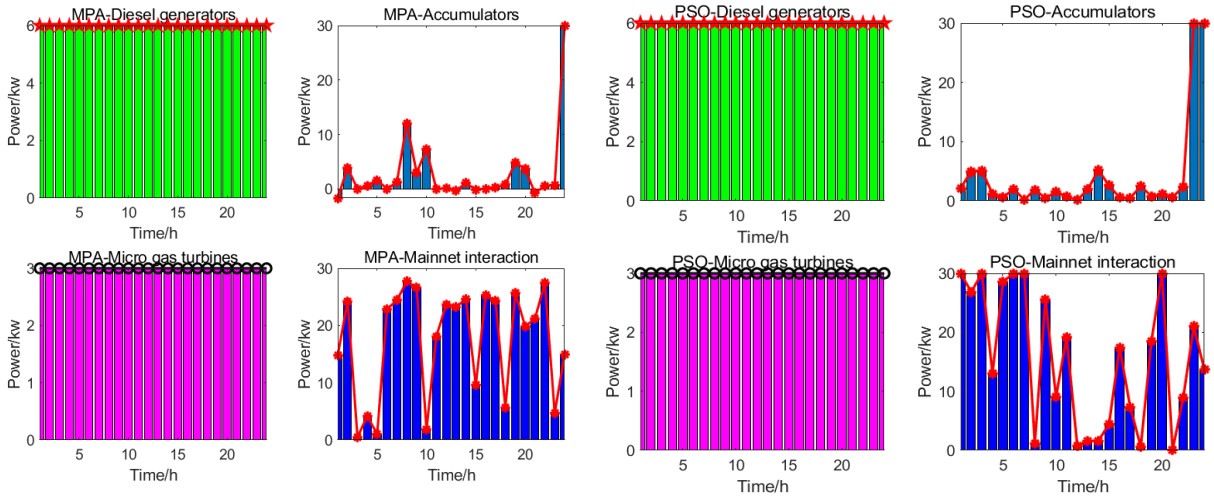

(g) MPA (h) PSO

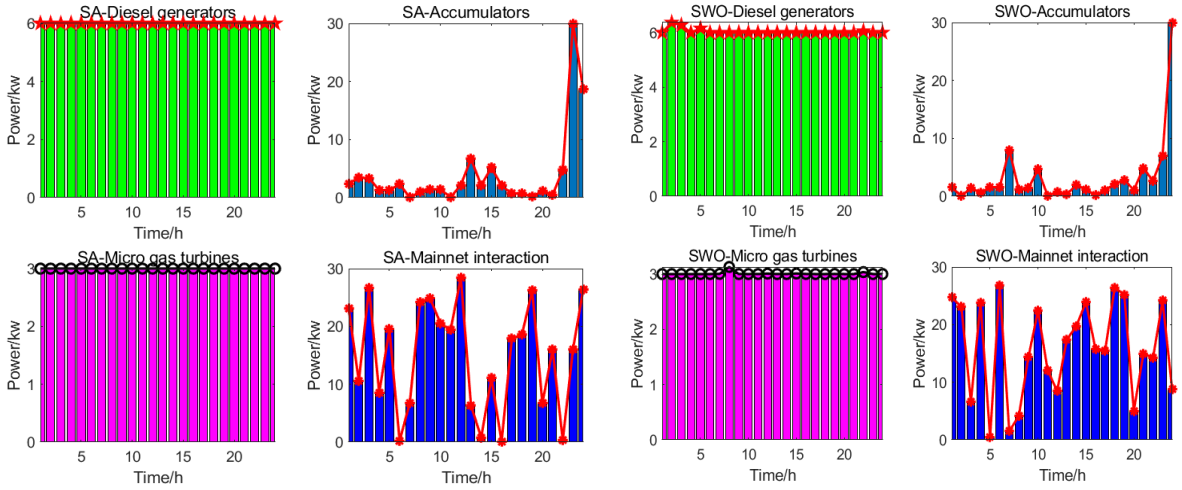

(i) SA (j) SWO

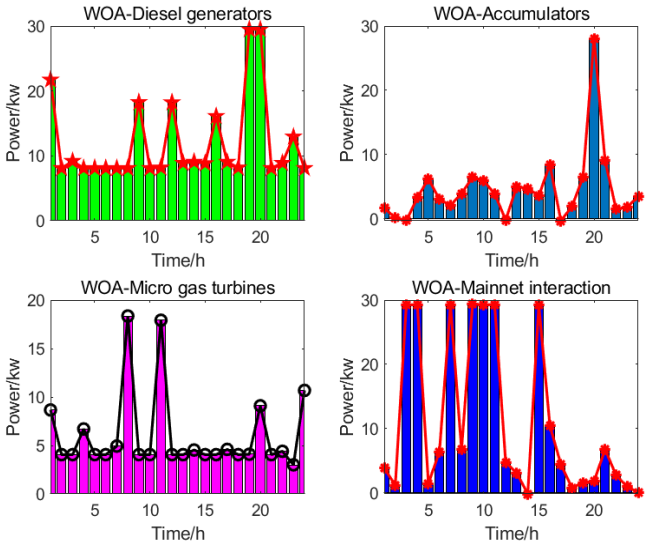

(k) WOA

Figure 6. *Unit power scheduling with the lowest total cost for each algorithm.*

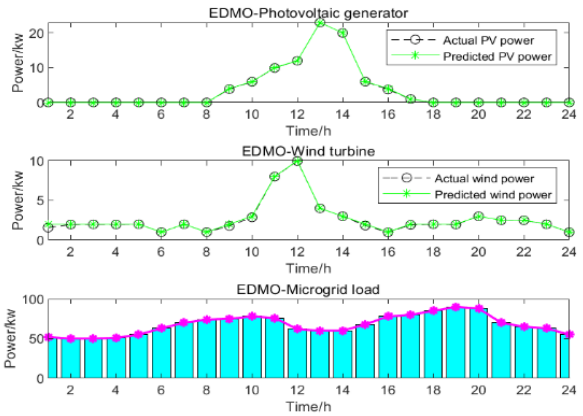

(a) EDMO

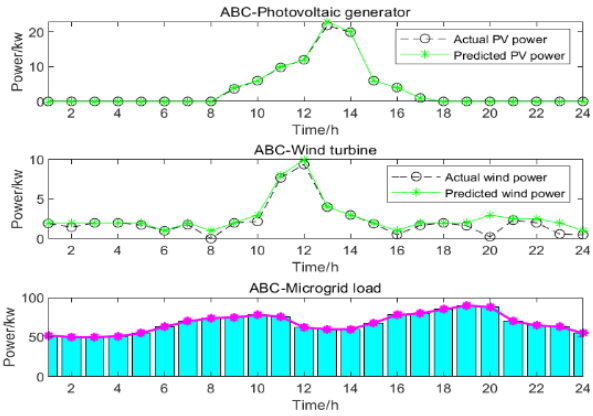

(b) ABC

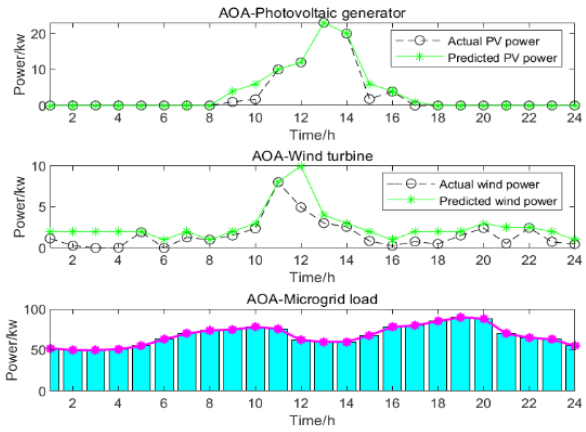

(c) AOA

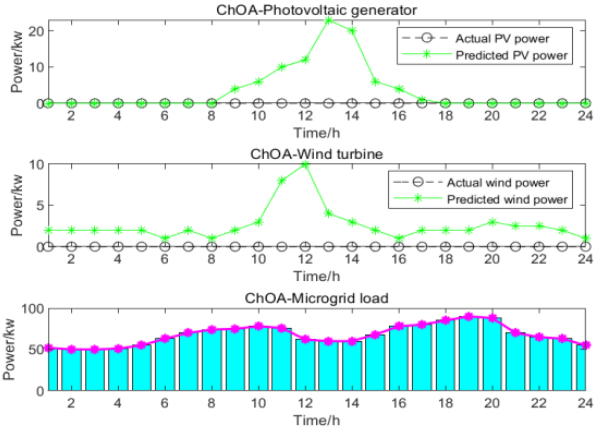

(d) ChOA

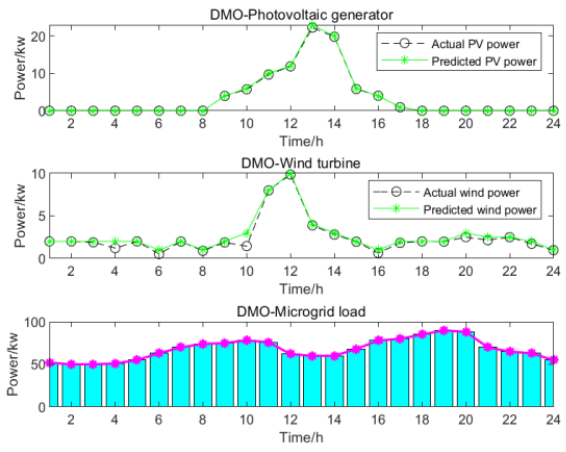

(e) DMO

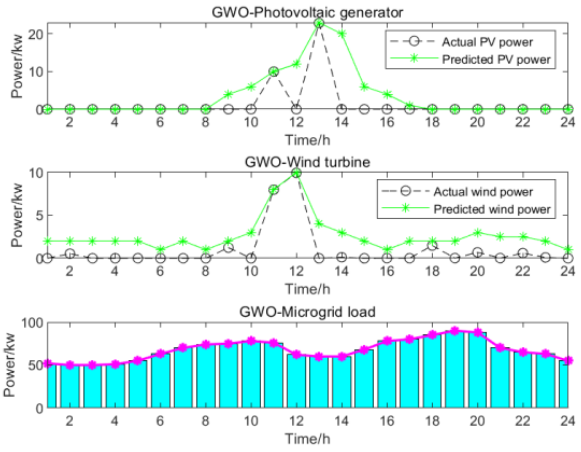

(f) GWO

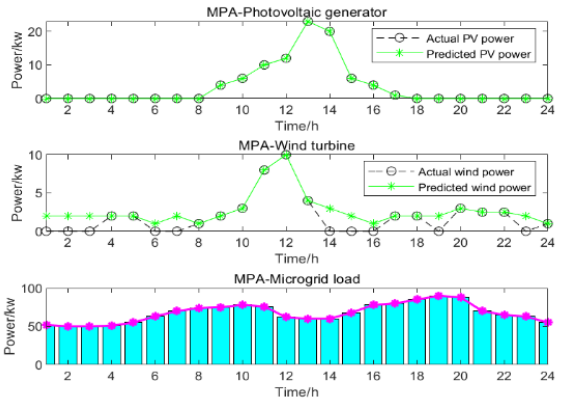

(g) MPA

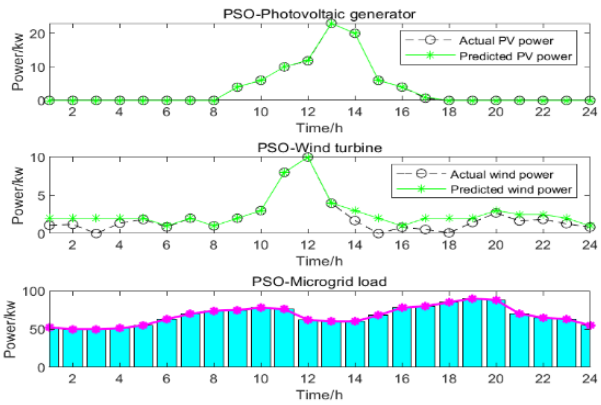

(h) PSO

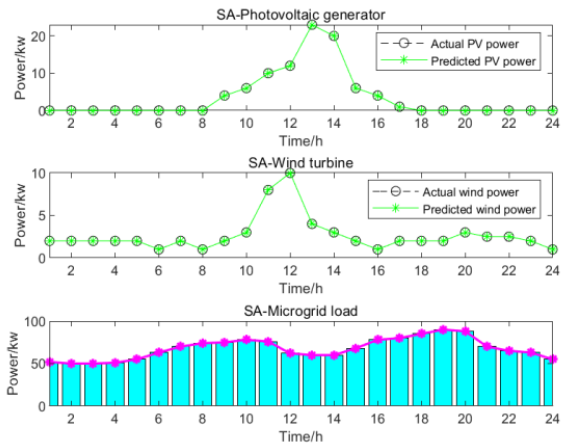

(i) SA

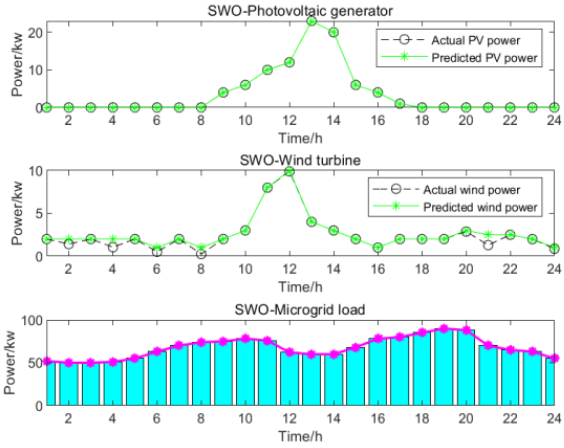

(j) SWO

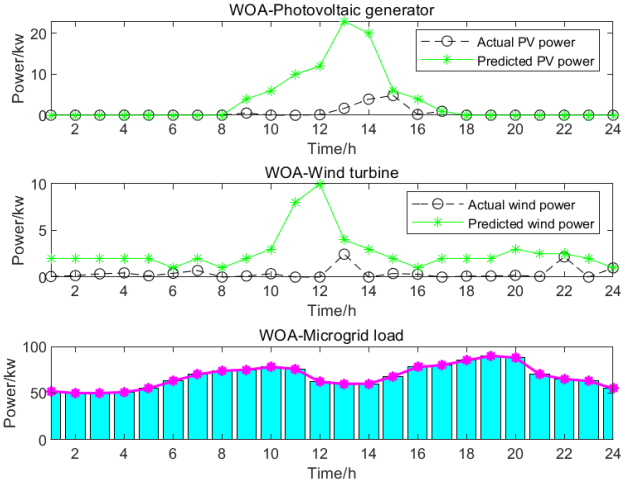

(k) WOA

Figure 7. *Fitting curves of the predicted values of each algorithm.*

Figure 5 shows the convergence graphs of each algorithm, from which it can be seen that EDMO obtains the minimum cost and converges faster. Figure 3 shows the scheduling results of each unit for EDMO with the minimum total cost, and Figure 4 shows the predicted values of PV, wind, and load power for EDMO with the minimum total cost. Figure 6 shows the unit power scheduling for each algorithm in the case of total cost minimization. Fig-

ure 7 shows the fitted curve plot of the predicted values of each algorithm, from which it can be seen that EDMO and SA have the best fit between the predicted and actual curves, and the predictive ability of EDMO basically matches the actual power generation, which verifies that EDMO has good predictive ability.

6. Conclusion and Future Work

For the microgrid optimal scheduling problem, this paper an EDMO is proposed. In the EDMO, the golden sinusoidal strategy is introduced, which utilizes the relationship between the sinusoidal function and the unit circle, searches the unit circle, and narrows the search space through the golden ratio to approximate the optimal solution of the algorithm. In addition, an adaptive t-distribution variation strategy was introduced to improve the population diversity in the late stage of the algorithm, and the L évy flight strategy was introduced to enhance the ability of the algorithm to jump out of the local optimum. The EDMO was applied to the microgrid optimal scheduling problem. The experimental results show that the EDMO yields the least costly economic scheduling scheme compared to other well-known algorithms, it can accurately predict the generation power of each unit. According to the Wilcoxon signed-rank test, EDMO exhibits good robustness and excellent optimization-finding ability. Therefore, the validity and superior performance of EDMO for solving the microgrid optimal scheduling problem is verified, and it is an effective alternative method for solving this problem. In future work, other strategies will be to improve the performance of the proposed algorithm to solve problems in other energy fields.

Abbreviations

EDMO	Enhanced Dwarf Mongoose Optimization
UC	Unit-combination
MG	Microgrid
QPSO	Quantum Particle Swarm Optimization
GA	Genetic Algorithm
MILP	Mixed-integer Linear Programming
GSA	Gravitational Search Algorithm
PSO	Particle Swarm Optimization
CSA	Cuckoo Search Algorithm
NSGA	Non-dominated Sorting Genetic Algorithm
WOA	Whale Optimization Algorithm
SOS	Symbiotic Organism Search
MA	Multi-intelligent Actor
IMACA	Improved Multi-intelligent Actor Consensus Algorithm
IBOA	Improved Butterfly Optimization Algorithm
GPC	Giza Pyramid Construction
NPC	Net Current Cost
LCOE	Levelized Cost of Energy
ATS	Adaptive t-distribution Mutation
MT	Microturbine
ABC	Artificial Bee Colony
AOA	Arithmetic Optimization Algorithm
ChOA	Chimp Optimization Algorithm
GWO	Grey Wolf Optimizer
MPA	Marine Predators Algorithm
SA	Simulated Annealing
SWO	Spider Wasp Optimizer.

Acknowledgments

This study was supported by the National Natural Science Foundation of China under Grant No. U21A20464.

Author Contributions

Weiping Meng wrote the original manuscript. Shijian Chen Algorithm Design. Yongquan Zhou Supervision, revised. All authors have read and approved the final manuscript.

Data Availability Statement

The authors were unable to specify which data were used.

Conflicts of Interest

The authors declare that they have no known competing financial interests or personal relationships that could have influenced the work reported in this study.

References

[1] Hernandez-Aramburo CA, Green TC, Mugniot N. Fuel consumption minimization of a microgrid. IEEE Trans Ind. Appl, 2005, 41(3): 673–81.

[2] Chen CL, Lee TY, Jan RM. Optimal wind–thermal coordination dispatch in isolated power systems with large integration of wind capacity. Energy Convers Manage 2006, 47: 3456–72.

[3] N. Karthik, A. K. Parvathy, R. Arul, A Review of Optimal Operation of Microgrids, International Journal of Electrical and Computer Engineering, 2020, 10(3): 2842–2849.

[4] Ping L, Xiangrui K, Chen F et al. Novel distributed state estimation method for AC - DC hybrid microgrids based on the Lagrangian relaxation method. Journal of Engineering, 2019(18): 4932-4936.

[5] Nemati M, Braun M, Tenbohlen S. Optimization of unit commitment and economic dispatch in microgrids based on genetic algorithm and mixed-integer linear programming. Applied energy, 2018, 210: 944-963.

[6] Halim, A. Hanif, Idris Ismail, Swagatam Das. Performance assessment of metaheuristic optimization algorithms: An exhaustive review. Artificial Intelligence Review, 2021, 54(3): 2323-2409.

[7] Xin-gang, et al. Economic-environmental dispatch of microgrids based on improved quantum particle swarm optimization. Energy, 2020, 195: 117014.

[8] Zhang, Xizheng, Zeyu Wang, Zhangyu Lu. Multi-objective load dispatch for microgrids with electric vehicles using a modified gravitational search and particle swarm optimization algorithm. Applied Energy, 2022, 306: 118018.

[9] Dong Y, Zhang Z, Hong W-C. A hybrid seasonal mechanism with a chaotic cuckoo search algorithm and a support vector regression model is used for electric load forecasting. Energies. 2018, 11(4): 1009.

[10] Nagarajan, et al. The combined economic emission dispatch of microgrids with the incorporation of renewable energy sources using an improved mayfly optimization algorithm. Computational Intelligence and Neuroscience 2022 (2022).

[11] S. Vasanthakumar, N. Kumarappan, R. Arulraj and T. Vigneysh, Cuckoo Search Algorithm based environmental economic dispatch of microgrid system with distributed generation, 2015 International Conference on Smart Technologies and Management for Computing, Communication, Controls, Energy and Materials (ICSTM), Avadi, India, 2015, pp. 575-580.

[12] Cheng, Shan et al. Dynamic dispatch optimization of the microgrid based on the QS-PSO algorithm. Journal of Renewable and Sustainable Energy 2017, 9, 4.

[13] Somakumar, et al. Optimization of emission cost and economic analysis for microgrids by considering a metaheuristic algorithm-assisted dispatch model. International Journal of Numerical Modelling: Electronic Networks, Devices and Fields 35.4 (2022): e2993.

[14] Zhao, Fei, Jinsha Yuan, Ning Wang. Dynamic economic dispatch model of a microgrid containing energy storage components based on a variant of the NSGA-II algorithm. Energies, 2019, 12(5): 871.

[15] Ma, Xiaoyan et al. Multi-objective microgrid optimal dispatching based on improved bird swarm algorithm. Global Energy Interconnection, 2022, 5(2): 154-167.

[16] Liao, Ching. Solve environmental economic dispatch of Smart Microgrids containing distributed generation systems–Using a chaotic quantum genetic algorithm. International Journal of Electrical Power & Energy Systems, 2012, 43(1): 779-787.

[17] Yang, Kang et al. Energy dispatch optimization of islanded multi-microgrids based on symbiotic organism search and improved multi-agent consensus algorithm. Energy, 2022, 239: 122105.

[18] Zhang, Hao, Guanghua Li, Shitong Wang. Optimization dispatching of isolated island microgrids based on the improved particle swarm optimization algorithm. Energy Reports, 2022, 8: 420-428.

[19] Zhang, Yu, et al. Research on economically optimal dispatching of microgrids based on an improved butterfly optimization algorithm. International Transactions on Electrical Energy Systems, 2022 (2022).

[20] M. Kharrich, S. Kamel, A. S. Alghamdi et al., Optimal design of an isolated hybrid microgrid for enhanced deployment of enewable energy sources in Saudi Arabia, Sustainability, 2021, 13(9): 4708.

[21] K. Zervoudakis, S. TsafarakisA. Mayfly optimization algorithm. Computers and Industrial Engineering, Vol. 145, Article ID 106559, 2020.

[22] Lacal-Arantegui R. Materials used in electricity generators in wind turbines state-of-the-art and future specifications. Journal of Cleaner Production, 2015. 87: 275-283.

[23] Lasnier F, Ang TG. Photovoltaic engineering handbook. Adam Hilger, New York IOP Publishing Ltd., 1990.

[24] Zhu J. Optimization of power system operation. John Wiley and Sons (2015).

[25] Mohamed Faisal A, Heikki N. System modelling and online optimal management of microgrid using mesh adaptive direct search. Int J Electric Power Energy Syst 2010; 32(5): 398–407.

[26] Campanari S, Macchi E. Technical and tariff scenarios effect on microturbine trigenerative applications. J Eng Gas Turb Power, 2004, 126: 581–589.

[27] Staffell, Review of small stationary fuel-cell performance. University of Birmingham; 2009.

[28] Jeffrey O. Agushaka, Absalom E. Ezugwu, Laith Abualigah, Dwarf Mongoose Optimization Algorithm, Computer Methods in Applied Mechanics and Engineering, 2022, 391: 114570.

[29] Tanyildizi E, Demir G. Golden Sine Algorithm: A Novel Math-Inspired Algorithm. Advances in Electrical & Computer Engineering 2017, 17(2): 71-78.

[30] Zhang H, Huang Q, Ma L et al. Sparrow search algorithm with adaptive t distribution for multi-objective low-carbon multimodal transportation planning problem with fuzzy demand and fuzzy time. Expert Systems with Applications 2024, 238: 122042.

[31] Kaidi W, Khishe M, Mohammadi M. Dynamic levy flight chimp optimization. Knowledge-Based Systems, 2022, 235–107625.

[32] Karaboga D. Artificial Bee Colony Algorithm. scholarpedia, 2010, 5(3): 6915.

[33] Abualigah L, Diabat A, Mirjalili S et al. Arithmetic optimization algorithm. Computer Methods in Applied Mechanics and Engineering, 2021, 376: 113609.

[34] Khishe M, Mosavi M: Chimp optimization algorithm. Expert Systems with applications, 2020149: 113338.

[35] Mirjalili S, Mirjalili S M, Lewis A. Grey wolf optimizer. Advances in engineering software, 2014, 69: 46-61.

[36] Faramarzi A, Heidarinejad M, Mirjalili S et al. Marine Predators Algorithm: Nature-inspired metaheuristic. Expert Systems with applications, 2020, 152: 113377.

[37] Kennedy J, Eberhart R. Particle Swarm Optimization. ICNN95-international Conference on Neural Networks. IEEE, 2002.

[38] Johnson D S, Aragon C R, Mcgeoch L A, et al. Optimization by Simulated Annealing: An Experimental Evaluation; Part I, Graph Partitioning. Operations Research, 1989, 37(6): 865-892.

[39] Abdel-Basset M, Mohamed R, Jameel M et al. Spider wasp optimizer: novel meta-heuristic optimization algorithm. Artificial Intelligence Review, 2023: 1-64.

[40] Mirjalili S, Lewis, A. Whale optimization algorithm. Advances in Engineering Software, 2016, 95: 51-67.

[41] Sallam, Karam M., et al. Improved gaining-sharing knowledge algorithm for parameter extraction of photovoltaic models. Energy Conversion and Management, 2021, 237: 114030.